Double diffraction stack for an alternative strategy for CRS-based limited-aperture Kirchhoff depth migration

Ines Veile, Geophysical Institute, University of Karlsruhe, Germany
Jürgen Mann*, Geophysical Institute, University of Karlsruhe, Germany

This paper was prepared for presentation at the 11th International Congress of The Brazilian Geophysical Society held in Salvador, Brazil, August 24-28 2009.

Summary

In Kirchhoff migration, the proper choice of the aperture is essential: the optimum aperture is the limited aperture defined by the first projected Fresnel zone. This is the smallest aperture providing interpretable amplitudes along with the highest possible S/N ratio and the minimum number of required summations. In addition, limited-aperture migration naturally prevents operator aliasing. The common-reflection-surface (CRS) stack provides kinematic wavefield attributes which allow to estimate the optimum aperture size for zero-offset and its dislocation with varying offset. The aperture is centered around the stationary point, but this point has to be associated with the corresponding point in the migrated domain in an additional process. Kirchhoff migration itself implicitly connects the stationary point and the image point in depth by collecting the energy in the vicinity of the former and assigning it to the latter. In principle, any smoothly varying property can be migrated "on top" of the seismic data themselves by applying multiple weighted diffraction stacks. The most generic property to be migrated in this way is the source/receiver midpoint which yields the lateral position of the stationary point mapped to the image location in depth. We investigate the validity and accuracy of this approach for simple synthetic data and apply it to a real land data set. A straightforward extension is introduced to solve some of the numerical problems inherent to this approach and CRS-based strategies are transferred from the time domain to the depth domain to identify the reflector images and to attenuate migration noise. Finally, the approach is compared to another CRS-based approach which directly evaluates the tangency criterion.

Introduction

In Kirchhoff migration the migrated time or depth image is generated by a summation along the forward-calculated diffraction traveltime surfaces (or Huygens surfaces) in the unmigrated domain. From a theoretical point of view, this summation has to be performed within an infinite aperture. Practically, the aperture is limited by the acquisition geometry, the recording time, and the computational costs. Schleicher et al. (1997) showed that the optimum limited aperture is the minimum aperture defined by the first projected Fresnel zone. Together with appropriate tapering within the adjacent second projected Fresnel zone, this yields interpretable amplitudes along the reflector images and the minimum number of required summations. As the summation is only carried out where the reflection event and the migration operator are virtually tangent to each other, this approach automatically prevents operator aliasing and minimizes the unwanted contributions from other events and background noise usually gathered along the remaining, non-tangent part of the migration operator.

The common-reflection-surface stack method (see, e. g., Mann et al., 1999; Jäger et al., 2001) provides kinematic wavefield attributes which allow to estimate various properties relevant for Kirchhoff migration: the geometrical spreading factor required for true-amplitude migration, as well as the projected Fresnel zone for zero-offset and the common-reflection-point (CRP) trajectory describing the dislocation of the stationary point with varying offset. The latter two are well suited to estimate the size of the limited aperture and its dislocation with offset. However, the absolute location of the aperture, the stationary point, has to be associated with the corresponding depth point in the migrated domain to actually perform limited-aperture Kirchhoff migration.

One strategy to determine the stationary point associated with a given image location in the migrated domain is to directly evaluate the tangency criterion between the migration operator and the reflection event. For the latter, the dip for offset zero is available from the CRS wavefield attributes such that the problem reduces to the determination of the migration operator dip for zero offset. In the next step, the stationary point found for offset zero is extrapolated along the CRP trajectory to finite offsets. Spinner and Mann (2005, 2006) used this concept in true-amplitude limited-aperture time migration. Based on a straight ray approximation, the required operator dip can be directly calculated from the analytic migration operator in this case. In contrast, for depth migration the migration operator will, in general, be of complex shape and an analytic approximation is no longer appropriate. To follow the tangency-based strategy here, Jäger (2005a,b) proposed to numerically calculate the migration operator dip by means of a finite-difference scheme from the Green's function tables (GFTs) on the fly during migration. Obviously, this approach is quite sensitive to the smoothness of the GFTs and, thus, to the smoothness of the underlying macro-velocity model.

In this contribution we want to investigate whether Kirchhoff migration itself is also suited to determine the stationary points in a stable and reliable way. Kirchhoff migration itself is far less sensitive to the smoothness of the GFTs than an operator dip calculated with the finite-difference scheme. Kirchhoff migration is a linear process. In addition, Kirchhoff migration only generates a significant output amplitude if a stationary point exists in the unmigrated domain. This implies that under certain conditions, a *local* scaling or weighting can be migrated "on top" of the seismic data. The most generic property to be migrated in this way is the source/receiver midpoint which directly yields the lateral location stationary point as a function of the image location.

In the following, we investigate the validity and accuracy of this so-called double diffraction stack approach for the determination of the stationary point with very simple synthetic data to identify the problems inherent to this approach. Based on this observations, we introduce an extended workflow which overcomes most of the encountered problems and apply it to a real land data set.

Double diffraction stack

Tygel et al. (1993) established the so-called double diffraction stack. Originally, it was intended to economize true-amplitude migration. We will show that this method is also able to support the CRS-based limited-aperture Kirchhoff migration.

Let us briefly review the basics of the diffraction stack method. For the sake of simplicity considering a planar measurement surface, each source location and each receiver location is defined by the parameter vector $\vec{\xi} = (\xi_1, \xi_2)$ that is confined to the aperture A. Using a given macro-velocity model, the traveltimes from each source or receiver to all points in the target zone are computed. This allows to calculate the diffraction traveltime t_D for any source/receiver combination associated with a given $\vec{\xi}$ with respect to a given depth point M, i. e., the Huygens surface $t_D\left(\vec{\xi}, M\right)$. The actual diffraction stack is then based on a summation along this Huygens surface in the prestack data. The output

$$V_j(M) = -\frac{1}{2\pi} \iint_A d\xi_1 d\xi_2 w_j\left(\vec{\xi}, M\right) \times \dot{U}\left(\vec{\xi}, t\right)\Big|_{t=t_D\left(\vec{\xi}, M\right)}$$

yields only a significant value if the point M lies close to a reflector. The time derivative (or half derivative in 2.5D) of U is required to restore the original wavelet. The weight w_j can be chosen such that it compensates for geometrical spreading in a true-amplitude migration. For a purely kinematic migration $w_j = 1$.

In principle, we can use any kind of weighting w_j during migration, provided that the weight function is smoothly varying with $\vec{\xi}$. According to the method of stationary phase (Bleistein, 1984), we will only receive contributions from the vicinity of the stationary point, of course, requiring appropriate tapering. Due to to the linearity of the migration process, the migration result will be locally weighted with the weight w_j applied at the stationary point. This leads to the general idea of the double diffraction stack, i. e., to perform Kirchhoff migration twice with two different weights, once with unit weight and once with a weight that carries the desired superimposed information. The ratio of the two migration results recovers the superimposed information at the migrated location. Since we try to find a reliable method to determine the stationary point which is characterized by the trace location it stands to reason that the trace location is used as the second migration weight. Accordingly, the ratio of the migration results directly represents the lateral locations of the stationary points.

In practice, we have to consider that the double diffraction stack results are only valid and reliable along reflector images. The structure of the data accounts for the correct positioning of the result. One consequence is that it is completely impossible to migrate the weight function without the underlying seismic data. In addition, we need criteria to decide where the stationary point is well defined. Numerically, we can expect that the approach is impeded by unstable results at locations with small amplitudes in both diffraction stack results, e. g., at zero crossings of the wavelet.

Synthetic data example

In this section we investigate a very simple synthetic data set to get some idea of the area in which the stationary point is valid and of its sensitivity with respect to the overall noise level. The model consists of two horizontal reflectors at depths of 1000 m and 2500 m with the same reflectivity embedded in a homogeneous background model with a velocity of 2000 m/s. This model definition has several advantages in this context:

- Migration is possible using analytical operators. Thus, potential errors in the macro-velocity model or in the corresponding GFTs cannot occur.
- The flat reflectors allow to use small migration apertures to exclude the risk of operator aliasing.
- Amplitudes can be extracted from the migration results along well-defined constant depth levels. Explicit picking and tracking of the events is not required.
- Due to its 1D nature, the stationary point should just represent the image location where it is defined. In other words, the relative displacement of this locations is a direct indicator of the obtained error.

For this model, we simulated a ZO data set with the primary reflection responses consisting of 351 traces with a sampling interval of 4 ms and a shot spacing of 20 m. The signal is a Ricker wavelet with a peak frequency of 40 Hz. Note that despite the identical reflectivity of the reflectors, the second reflection event appears far weaker due to the larger geometrical spreading. Colored noise of various different levels[1] has been superimposed to the data.

Each seismic trace has been multiplied with its shot position to obtain the weighted input for the double diffraction stack. Poststack Kirchhoff migration was applied to the unweighted data and the weighted data, with a target zone of 5000 m width and 3000 m depth at sampling rates of 20 m and 5 m, respectively. The aperture linearly varies between 100 m and 500 m with increasing target depth. Finally, we computed the ratio of the two migration results to recover the stationary point. In the resulting section (not displayed), the lateral location of the stationary point seems to closely follow the lateral image location, even in the noisy areas in between the two reflector images! The latter phenomenon can be easily explained: the used aperture is symmetric with respect to the considered lateral image location. In the noisy areas, the migration effectively averages all trace locations within the aperture with random weighting factors.

[1] In this contribution S/N ratio refers to the correspondent parameter of the Seismic Un*x (Cohen and Stockwell, 2000) utility `suaddnoise`.

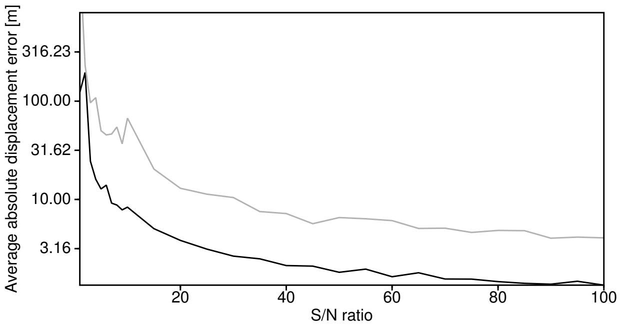

Figure 1: Synthetic data: semilogarithmic display of the average absolute displacement error for the first (black) reflector and the second (gray) reflector.

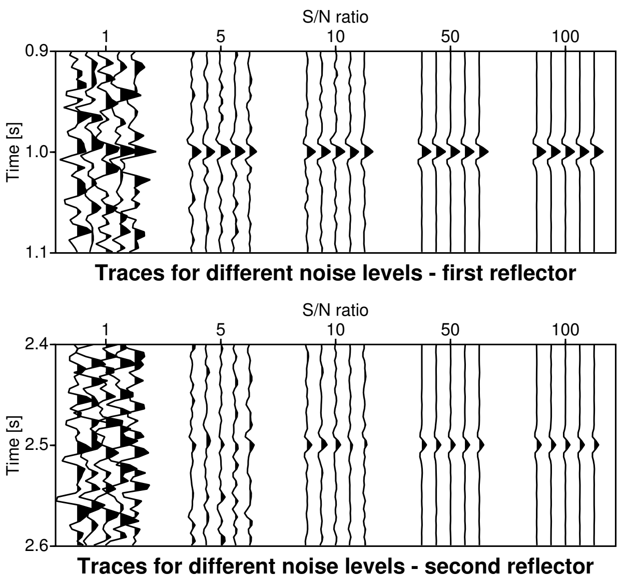

Figure 2: Synthetic data: representative traces for different noise levels for the first reflector (top) and the second reflector (bottom).

This average scatters around the unweighted average, i. e., the center of the aperture which coincides with the lateral image location.

Obviously, this way of analyzing the results is of little use as the large variation of the weight function along the entire section completely obscures any local variations. For this 1D model, the actual stationary point along the reflector images should coincide with the lateral image location. Thus, a section of the *relative* displacement between the lateral location of the stationary locations and the lateral position of the depth image point is far better suited to analyze the validity and accuracy of the results. In this representation (also not displayed) it is evident that the result in the noisy areas is as random as expected, whereas the result along the reflector images is close to the expected zero displacement. Thus, an identification of the reflector images is mandatory to decide whether the double diffraction stack result is valid at a given depth location.

For a systematic analysis of this displacement as a function of the S/N ratio and the position within the wavelet, we consider the average absolute displacement error along constant depth levels. For the center of the Ricker wavelet, the average absolute displacement error is displayed in Figure 1 for various noise levels. For illustration, Figure 2 shows some representative traces for different noise levels. For reasonably high S/N ratios, the average error is is far smaller than the size of the first projected Fresnel[2] zone, which is ≈ 320 m for the first reflector and ≈ 500 m for the second reflector. However, there is a certain error remaining even for very high S/N ratios which can be attributed to migration noise. The attenuation of this migration noise will be addressed later.

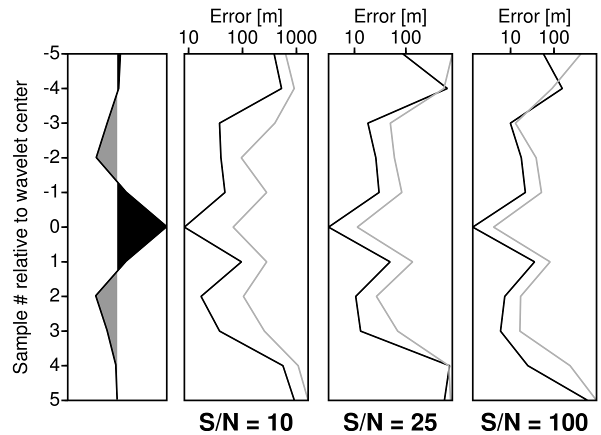

Figure 3: Synthetic data: left: migrated Ricker wavelet (without noise). Right: semilogarithmic representation of the average absolute displacement error along the wavelet for the first reflector (black) and the second reflector (gray) for three different noise levels. Note the different horizontal scales. Depth sampling interval is 5 m.

In the next step, we analyze the average absolute displacement error in a similar manner along the seismic wavelet. Figure 3 displays this error as a function of the distance to the center of the wavelet for three different noise levels together with the original, noise-free wavelet. We can clearly observe that the error varies significantly along the wavelet. Especially at zero crossings, the error strongly increases. This directly reflects the expected numerical problems occurring for small amplitudes in the both migrations results used to compute the stationary points. As the displacement errors quickly exceed any acceptable limit, i. e., the size of the projected first Fresnel zone at such locations, we will address this problem in the real data example below.

Real land data example

The 2D seismic land dataset discussed in the following was acquired by an energy resource company in a fixed-spread geometry. The seismic line has a total length of about 12 km. The utilized source signal was a linear upsweep from 12 to 100 Hz of 10 s duration. Shot and receiver spacing are both 50 m and the temporal sampling interval is 2 ms. Standard preprocessing was applied to the field data including the setup of the data geometry, trace editing, deconvolution, geometrical spreading correction, field static correction, and bandpass filtering. The underlying struc-

[2] Calculated for a monochromatic signal of 40 Hz. Of course, the ZO projected Fresnel zone coincides with the interface Fresnel zone for this 1D model.

ture consists of slightly dipping layers interrupted by faults in some parts. An entire imaging sequence consisting of CRS stack, normal-incidence-point-wave tomography, and limited-aperture poststack and prestack Kirchhoff migration for these data can be found in Hertweck et al. (2004) and Hertweck (2004). We used the same CRS-stacked section and the same GFTs for the application of the double diffraction stack. All migration parameters have been pertained to make the results comparable: the target grid is sampled with 20 m in lateral direction and 4 m in vertical direction. The symmetric aperture has an half-width varying from 60 m to 450 m from top to bottom.

As for the synthetic data, we weighted each trace of the input data, here the CRS stack result, with its shot location. Two independent Kirchhoff poststack migrations have been performed, one of the weighted input and one of the unweighted input, respectively. Figure 4 shows the migration result for the unweighted input together with the ratio of the two migration results. Again, the direct display of the stationary point is quite pointless as it does not provide the required resolution. The same applies to similar double diffraction stack results as, e. g., presented by Chen (2004). To obtain an interpretable result, we again calculated the relative lateral displacement of the stationary point with respect to the image location in depth. In contrast to our synthetic example where the exact displacement is zero, this displacement will, in general, not vanish for the real data: Figure 4 (bottom) shows this displacement with an obvious correlation to the dip of the reflector images: we can directly observe the lateral component of the well-known up-dip movement during migration. Furthermore, we encounter the expected instabilities at zero-crossings, some background migration noise, and various regions where the results are obviously meaningless. Our first aim is to remove this instabilities and to attenuate the migration noise. The corresponding result is displayed in Figure 5. Finally, the depth locations with meaningful results have to identified. In the following, we will discuss the individual employed processing steps and demonstrate their effects for a subset of the migration target zone:

Instabilities at zero-crossings. As can be seen in Figure 6b, the stationary point gets unacceptably inaccurate at zero-crossings of the wavelet. In its original form, i. e., the ratio of the diffraction stack results, the accuracy of the stationary point is below reasonable limits and, thus, of no practical use. Unfortunately, other publications on double diffraction stack like Chen (2004) do not comment on this problem and its solution. To overcome these numerical problems occurring at zero-crossings we have to get rid of the corresponding phase behavior of the wavelet. This can be achieved in a strikingly straightforward way if we calculate the envelope of the analytic signal for both diffraction stack results *before* computing their ratio. Naturally, the envelope is non-zero along the entire wavelet. Therefore, the numerical problems should completely disappear. Indeed, this can be readily seen in Figure 6c: the displacement of the stationary point is now stable along the entire wavelet.

Identification of reflector images. The double diffraction stack result is only well-defined along actual reflector images. Therefore, we have to identify the latter to select the locations associated with meaningful results. For that purpose, we have transferred the CRS stacking strategy from the time domain to the depth domain: originally designed to detect and parameterize reflection events in the unmigrated prestack time domain up to second order based

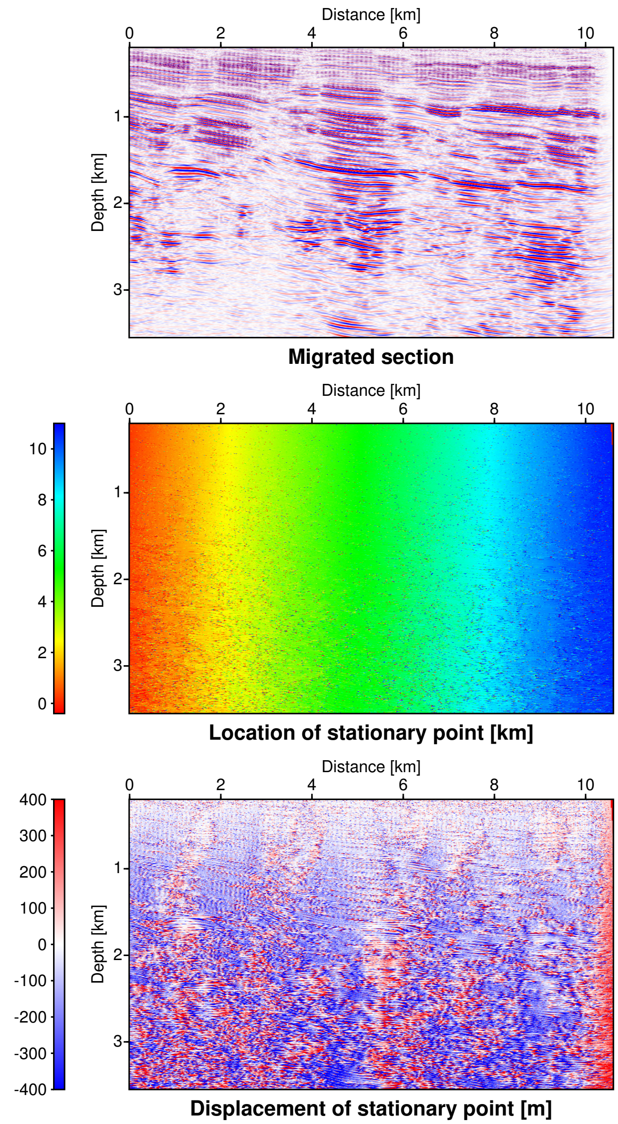

Figure 4: Real land data: top: unweighted poststack depth migration result. Middle: lateral location of the stationary point given by the ratio of the double diffraction stack results. Bottom: relative lateral displacement between the stationary point and the depth image point.

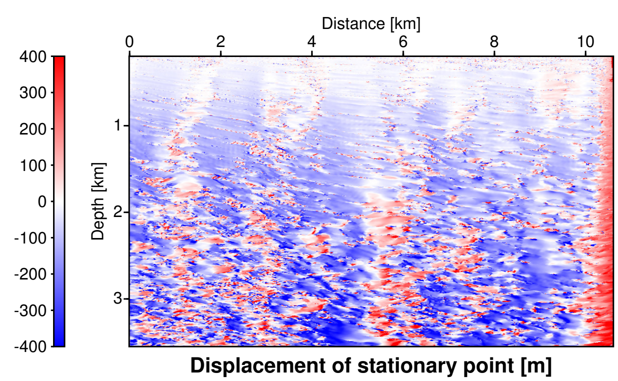

Figure 5: Real land data: relative lateral displacement between the stationary point and the depth image point after final processing.

on coherence analysis, we applied the same strategy in the migrated poststack domain. At each depth location, we determine the hyperbolic trajectory along which coherence analysis in the migration result yields the highest coherence value. In this way we parameterize the reflector images in terms of their local dip and curvature. For points not located on an actual reflector image, the coherence value will be low and allows to discriminate between reflector images and noise. A coherence threshold has been used for this purpose to mask out the meaningless values in Figures 6b to d.

Attenuation of migration noise. The high-frequency variation of the double diffraction stack result is not consistent with ray theory which predicts a smooth variation along the reflector images. Thus, this effect has to be considered as unwanted migration noise and should be filtered along the reflector images. Again, strategies developed in the framework of the CRS stack can be readily adapted for this task: Mann and Duveneck (2004) proposed an event-consistent smoothing strategy to remove similar unphysical fluctuations from CRS wavefield attributes. The strategy uses coherence values and locals dips of the events to select the samples belonging to the same event, i. e., to ensure event consistency, and applies a combined median and averaging filter to the selected samples. Fortunately, the required dips and coherence values are already available from the identification of the reflector images such that the smoothing algorithm can be directly applied. The result shown in Figure 6d reveals a strong attenuation of the migration noise.

With the just described tools, we can define a workflow to determine the stationary points and their reliability:

- weight each input trace with its location
- perform double diffraction stack
- calculate envelope of analytic signal in both results
- calculate ratio of both results
- apply "CRS stack" in poststack migrated depth domain
- use coherence section to select meaningful data
- perform event-consistent smoothing using local dip and coherence

Finally, we can compare the stationary points obtained with this workflow with the corresponding results based on the direct evaluation of the tangency criterion proposed by Jäger (2005a,b). Figure 7 shows a subset of the conventional migration result. For the trace in its center, the lateral displacement between stationary points and the image points is displayed along with the size of the projected first Fresnel zone for both approaches. The latter allows to relate the fluctuations and potential errors in the displacement, i. e., in the relative position of the migration aperture, to the aperture size. Apart from the discrete nature of the dip-based approach, the result of the double diffraction stack appears more reasonable: its fluctuations are well below the Fresnel zone size and follow a consistent trend, whereas the former shows stronger fluctuations, especially at smaller depths. In this case study, the almost 1D nature of the considered data set largely tolerates such errors. However, this might not hold for more complex situations.

Conclusions

We have revisited the double diffraction stack approach proposed by Tygel et al. (1993). In this paper, our intention is to use it as a simple and efficient method to calculate the relation between the stationary point in the unmigrated domain and the corresponding image point in the depth-migrated domain. In principle, this allows to correctly place the migration aperture in limited-aperture migration and to extract the CRS wavefield attributes defined at the stationary point. These attributes provide information on the aperture size and its behavior with varying offset and, thus, all information required to perform limited-aperture migration (see, e. g., Jäger, 2005a; Spinner and Mann, 2005).

The direct calculation of the stationary point as ratio of the two diffraction stack results turned out to be unstable and unreliable especially at zero-crossings of the wavelet. We addressed these numerical problems by using the envelope of the analytic signal and by transferring CRS strategies from the time domain to the depth domain. This allows to identify and parameterize reflector images and to apply CRS-based event-consistent smoothing. The presented case study demonstrates that the numerical problems can be successfully handled by this strategy. The stationary points determined in this way can then be used as an alternative to their counterparts computed according to the strategy proposed by Jäger (2005a).

Acknowledgments

We would like to thank the sponsors of the Wave Inversion Technology (WIT) Consortium for their continuous support.

References

Bleistein, N. (1984). *Mathematical methods for wave phenomena*. Academic Press Inc., San Diego.

Chen, J. (2004). Specular ray parameter extraction and stationary-phase migration. *Geophysics*, 69(1):249–256.

Cohen, J. K. and Stockwell, Jr., J. W. (2000). *CWP/SU: Seismic Un*x release 34: a free package for seismic research and processing*. Center for Wave Phenomena, Colorado School of Mines.

Hertweck, T. (2004). *True-amplitude Kirchhoff migration: analytical and geometrical considerations*. Logos Verlag, Berlin.

Hertweck, T., Jäger, C., Mann, J., Duveneck, E., and Heilmann, Z. (2004). A seismic reflection imaging workflow based on the Common-Reflection-Surface (CRS) stack: theoretical background and case study. In *Expanded Abstract, 74th Ann. Internat. Mtg.* Soc. Expl. Geophys. Session SP 4.3.

Jäger, C. (2005a). Minimum-aperture Kirchhoff migration by means of CRS attributes. In *Extended abstracts, 67th Conf.* Eur. Assn. Geosci. Eng. Session F042.

Jäger, C. (2005b). *Minimum-aperture Kirchhoff migration with CRS stack attributes*. Logos Verlag, Berlin.

Jäger, R., Mann, J., Höcht, G., and Hubral, P. (2001). Common-Reflection-Surface stack: image and attributes. *Geophysics*, 66(1):97–109.

Mann, J. (2002). *Extensions and applications of the Common-Reflection-Surface Stack method*. Logos Verlag, Berlin.

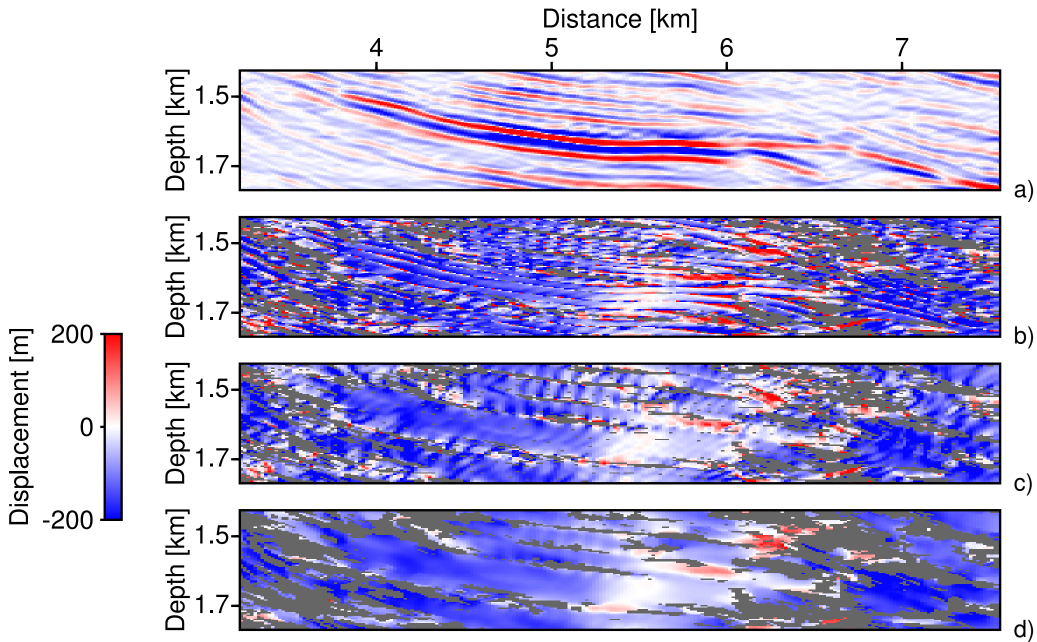

Figure 6: Real land data: a) detail of the migrated section, b) corresponding detail of the lateral displacement between image point and stationary point, c) dto., but displacement calculated from the envelopes of the migration results, d) section shown in c) after event-consistent smoothing. Values not located on reflector images have been masked out in gray.

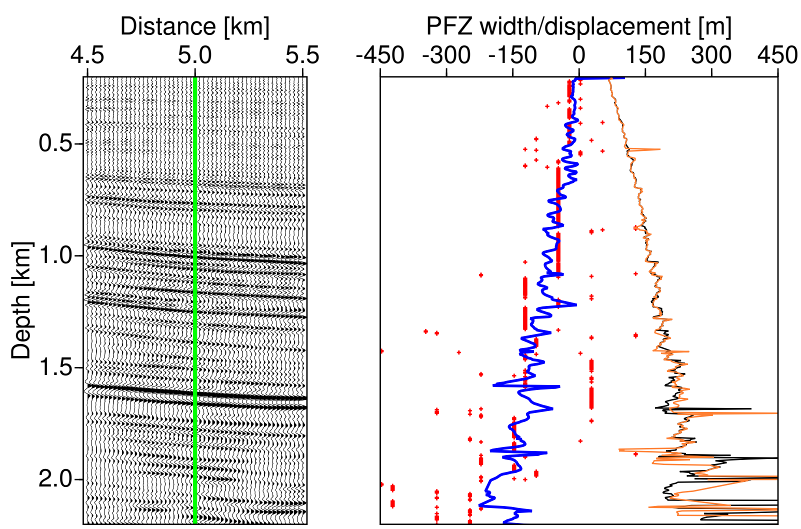

Figure 7: Real data set: left: subset of the migration result. The trace marked in green is used for the comparison of the two approaches. Right: lateral displacement between the stationary point and the depth image point obtained with the dip-based approach (red crosses) and the double diffraction stack (blue line). The size of the projected first Fresnel zone for ZO in the dip-based approach (black) and the double diffraction stack approach (brown).

Mann, J. and Duveneck, E. (2004). Event-consistent smoothing in generalized high-density velocity analysis. In *Expanded Abstracts, 74th Ann. Internat. Mtg.* Soc. Expl. Geophys. Session ST 1.1.

Mann, J., Jäger, R., Müller, T., Höcht, G., and Hubral, P. (1999). Common-Reflection-Surface stack – a real data example. *J. Appl. Geophys.*, 42(3,4):301–318.

Schleicher, J., Hubral, P., Tygel, M., and Jaya, M. S. (1997). Minimum apertures and Fresnel zones in migration and demigration. *Geophysics*, 62(1):183–194.

Spinner, M. and Mann, J. (2005). True-amplitude CRS-based Kirchhoff time migration for AVO analysis. In *Expanded abstracts, 75th Ann. Internat. Mtg.* Soc. Expl. Geophys. Session AVO 2.4.

Spinner, M. and Mann, J. (2006). True-amplitude CRS-based Kirchhoff time migration for AVO/AVA analysis. *J. Seis. Expl.*, 15(2):133–152.

Tygel, M., Schleicher, J., Hubral, P., and Hanitzsch, C. (1993). Multiple weights in diffraction stack migration. *Geophysics*, 59(12):1820–1830.